

See discussions, stats, and author profiles for this publication at: <https://www.researchgate.net/publication/265177485>

Some Aspects of Configuration Interaction of the $4f(N)$ Configurations of Tripositive Lanthanide Ions

ARTICLE in THE JOURNAL OF PHYSICAL CHEMISTRY A · AUGUST 2014

Impact Factor: 2.69 · DOI: 10.1021/jp507053v · Source: PubMed

CITATIONS

2

READS

102

3 AUTHORS:



Peter Anthony Tanner

The Hong Kong Institute of Education

355 PUBLICATIONS 4,367 CITATIONS

SEE PROFILE



Yau-yuen Yeung

The Hong Kong Institute of Education

85 PUBLICATIONS 1,080 CITATIONS

SEE PROFILE



Lixin Ning

Anhui Normal University

63 PUBLICATIONS 425 CITATIONS

SEE PROFILE

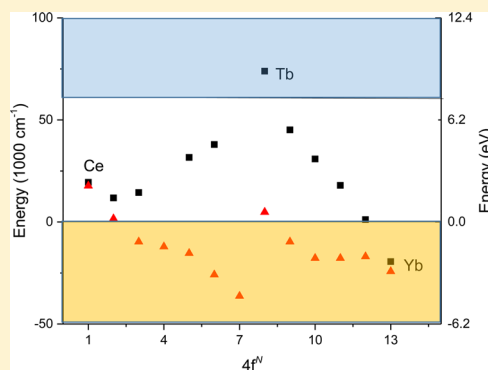
Some Aspects of Configuration Interaction of the $4f^N$ Configurations of Tripositive Lanthanide Ions

Peter A. Tanner,^{*,†} Yau-Yuen Yeung,[†] and Lixin Ning[‡]

[†]Department of Science and Environmental Studies, The Hong Kong Institute of Education, 10 Lo Ping Road, Tai Po, New Territories, Hong Kong S.A.R., People's Republic of China

[‡]Center for Nano Science and Technology, Department of Physics, Anhui Normal University, Wuhu, Anhui 241000, People's Republic of China

ABSTRACT: Some features of the interaction of the $4f^N$ configuration of tripositive lanthanide ions (Ln^{3+}) with excited configurations have been investigated. The calculated barycenter energies of the same parity $4f^{N-1}6p$, $4f^{N+1}5p^5$, and $4f^{N-1}5f$ configurations for Ln^{3+} , relative to those of $4f^N$, are fitted well by exponential functions. The $4f^N$ barycenter energies of Ln^{3+} in $\text{Y}_3\text{Al}_5\text{O}_{12}/\text{Ln}^{3+}$ lie in the band gap, with the exceptions of Tb^{3+} and Yb^{3+} , where they are situated in the conduction and valence bands, respectively. The configuration interaction parameters α , β , and γ , which are fitted in the usual phenomenological Hamiltonian to calculate the crystal field energies of Ln^{3+} , exhibit quite variable magnitudes in the literature due to incomplete energy level data sets, energy level misassignments and fitting errors. For $\text{LaCl}_3/\text{Ln}^{3+}$, 83% of the variation of α and 50% of that for β can be explained by the change in the difference in barycenter energy with the predominant interacting configuration. The parameter γ is strongly correlated with the Slater parameter F^2 and is not well-determined in most calculations. The values of the electrostatically correlated spin–other orbit parameter P^2 vary smoothly across the Ln^{3+} series with the barycenter difference between the $4f^N$ and $4f^{N-1}5f$ configurations. Calculations of the P^k ($k = 2, 4$, and 6) values for Pr^{3+} show that $4f \rightarrow nf$ excitations only account for $\sim 65\%$ of the value of P^2 for $\text{LaCl}_3/\text{Pr}^{3+}$ and 35% of that in $\text{Y}_3\text{Al}_5\text{O}_{12}/\text{Pr}^{3+}$. The role of the ligand is therefore important in determining the value, and a discussion is included of the present state of configuration-interaction-assisted crystal field calculations. Further progress cannot be made in the above areas until more reliable and complete energy level data sets are available for the Ln^{3+} series of ions in crystals.



1. INTRODUCTION

The tripositive lanthanide ions have the electronic configuration of $[\text{Xe}]4f^N$ ($N = 1$ for Ce^{3+} up to $N = 13$ for Yb^{3+}). The number of energy levels of the $4f^N$ configuration varies tremendously, from 7 Kramers doublets for Ce^{3+} and Yb^{3+} up to 3003 nondegenerate levels for Eu^{3+} and Tb^{3+} . The energies of these states are calculated most accurately by a phenomenological Hamiltonian, described in the Methodology section, which comprises atomic (H_{AT}) and crystal field (H_{CF}) terms. The atomic part describes the properties of the free ion (i.e., gaseous, uncoordinated ion) and comprises terms representing interelectronic repulsion between the $4f^N$ electrons (with parameters F^k , Slater integrals), the coupling between spin and orbital angular momenta (parameter ζ_{4f}), and terms describing the electrostatic configuration interaction (CI) with higher configurations (parameters α , β , and γ), as well as some additional terms.

The CI terms are an attempt to rectify the fact that the calculation of $4f^N$ energy levels cannot be accurately performed by just considering this configuration alone and that we should include all configurations in our model. Their inclusion makes the calculation much less complicated than the alternative multiconfigurational calculation. This latter approach has

indeed been employed in the calculation of J -multiplet terms of lanthanide free ions.¹ The correlation effects of $5s$, $5p$, $4f$, $5d$, and $6s$ electrons of Ln^{3+} have also been taken into account in a direct way by employing ab initio quantum chemical calculations (for example, refs 2 and 3), but the calculation error, even for J -multiplets of the $4f^2$ ion Pr^{3+} , can amount to several thousands of cm^{-1} .²

The linear theory of CI was introduced to account for the effects of higher perturbing configurations (for example, refer to ref 4). The effects of electrostatic perturbations from other configurations can be represented by corrections to the matrix elements of $4f^N$ involving the scalar products of odd-rank tensor operators. The corrections involving the corresponding even-rank operators are effectively already absorbed into and concealed in the Slater integrals. It was thought that the second-order effects of CI could be added linearly. The Hamiltonian H_{AT} could be augmented by two-body scalar terms for the terms with odd-rank operators, and these were replaced by an equivalent expression involving the parameters

Received: July 15, 2014

Revised: August 28, 2014

Published: August 29, 2014

α , β , and γ . Some types of CI have been described by Rajnak and Wybourne.⁵ These authors pinpointed five types of configuration that can modify the energy level structure of the $4f^N$ configuration ($1s^2 2s^2 2p^6 3s^2 3p^6 3d^{10} 4s^2 4p^6 4d^{10} 5s^2 5p^6 4f^N$), as exemplified, for example, by (a) $4f^{N-2}6s^2$ and $4f^{N-2}6s6d$; (b) $5p^4 4f^{N+2}$ and $4d^9 5s 4f^{N+2}$; (c) $5p^5 4f^{N+1}6p$; (d) $4f^{N-1}6p$; and (e) $5p^5 4f^{N+1}$, where (b), (c), and (e) are core excitations.⁵ Note that the interacting configuration must be of the same parity as $4f^N$, where parity can be even or odd, depending upon whether the sum of the one-electron angular momentum is even or odd, respectively. It would also be expected that the most important interactions occur for those configurations that only differ by the excitation of one or two electrons. Therefore, the next-highest configuration above $4f^N$ (i.e., $4f^{N-1}5d$) that has been extensively studied during the past 25 years (for example, refs 6–8) is not a candidate because it has opposite parity to $4f^N$. The same applies to the next-higher configuration, $4f^{N-1}6s$. Rajnak and Wybourne⁵ found that the correction to electrostatic matrix elements in H_{AT} for CI between $4f^N$ and $5p^5 4f^{N+1}$ and that between $4f^N$ and $4f6p$ contain nonlinear three-particle terms, in addition to two-body terms. Judd⁹ described the effective three-particle operators, with parameters T^k , and noted that the effective two-particle parts could be absorbed into the Casimir operators¹⁰ with the parameters α , β , and γ . These latter parameters also absorb the orbit–orbit interaction between electrons.¹¹ This interaction describes the fact that two electrons orbiting in the same direction (hence giving a large total orbital angular momentum) will encounter less often than those when orbiting in opposite directions and hence repel each other less.

Higher configurations of Ln^{3+} above $4f^{N-1}5d$ and $4f^{N-1}6s$ have received little attention. Enzonga Yoca and Quinet¹² have recently utilized a relativistic Hartree–Fock method to calculate oscillator strengths of emission transitions from higher configurations of the Nd^{3+} free ion and hence to provide energy level assignments. Meftah et al. have observed 760 lines in the free ion emission spectrum of Tm^{3+} , corresponding to transitions between 157 states.¹³ However, the NIST atomic database Website¹⁴ only lists some electron configuration information for Pr^{3+} , shown graphically in Figure 1. Hence, from this figure, $4f6p$ and $4f5f$ are configurations of the same parity as $4f^2$ and could be considered as candidates for CI, with $4f6p$ being of most importance in this case because the

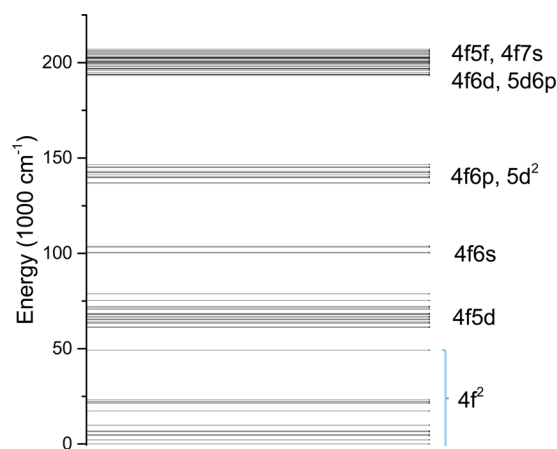


Figure 1. Energy levels of the Pr^{3+} free ion up to 206369 cm^{-1} . The ionization limit is at 314400 cm^{-1} . The $4f^N$ energies are taken from ref 18, and the energies of other configurations are extracted from ref 14.

interaction is inversely proportional to the energy difference between the configuration barycenters, $\Delta E(\text{bc})$. The barycenter of a configuration represents the degeneracy-weighted mean of the energy levels in the configuration.

Rajnak and Wybourne¹⁵ have also discussed the effects of higher configurations in modifying the spin–orbit interaction of a $4f^N$ configuration. Following the inclusion of effects described by the Breit equation approximation into the Hamiltonian,¹⁶ it has been customary to describe the parametrization of the electrostatically correlated spin–orbit interaction by three P^k parameters ($k = 2, 4$, and 6) and to use the Hartree–Fock ratios of $P^4 = 0.75P^2$, $P^6 = 0.5P^2$ so that the interaction is parametrized by only one parameter.¹⁷ Because the spin–orbit coupling interaction with the nucleus and core electrons is represented by a one-particle operator, a nonzero CI effect on it can only occur with the substitution of a single orbital of the same orbital quantum number.¹⁵

Recently,¹⁸ we found that the fitted values of the parameters α and β were linearly proportional to the inverse barycenter difference between the $4f^2$ configuration and the nearest one for the isoelectronic series La^{3+} , Ce^{3+} , Pr^{3+} , and Nd^{3+} . A major aim of the present paper was to observe to what extent this linear relation holds for the entire series of tripositive lanthanide ions. From our results, we hoped to observe whether the investigated parameters would vary in an accountable and systematic manner across the Ln^{3+} series, so that previously missing or erroneous values could be interpolated from our results.

2. METHODOLOGY

The calculation of energy levels for the $4f^N$ configuration is most accurately performed by a semiempirical Hamiltonian comprising atomic (H_{AT}) and crystal field (H_{CF}) components

$$H = E_{AVE} + H_{AT} + H_{CF} \quad (1)$$

$$H_{AT} = \sum_k F^k f_k + \sum_i \zeta_f \mathbf{s}_i \cdot \mathbf{l}_i + H_{ADD} \quad (2)$$

where $k = 2, 4$, and 6 , i represents the sum over all $4f$ electrons, and normal and bold fonts represent parameters and operators, respectively. The first term in eq 1, E_{AVE} , is the energy difference between the $4f^N$ configuration barycenter and its ground level. The electron kinetic energy and its electrostatic interactions with the nuclear charge and inner electrons are absorbed into the barycenter energy. Note that the matrix of H_{AT} is often made traceless in the actual fitting process by subtracting the average trace (i.e., the average of all of the diagonal matrix elements) from it. There is also a distinction between E_{AVE} and the Slater parameter F^0 , which can shift the position of the calculated barycenter but is usually not used in the fitting of energy levels. The Slater (F^k) and spin–orbit interaction (ζ_f) parameters have been described above. The additional terms, H_{ADD} , relevant to the present work are the two-body CI parameters (α , β , and γ) and the electrostatically correlated spin–orbit coupling parameters P^k ($k = 2, 4$, and 6). One of us (Y.Y. Yeung) has developed a user-friendly computer program to calculate and carry out least-squares fits of state energies of $4f^N$ configurations using the Hamiltonian eq 1. This program includes matrix elements describing spin–spin interactions,¹⁹ which have been omitted in most previous models, and its use has been described elsewhere.²⁰ The program has been employed for calculations of the energy parameters for $\text{Y}_3\text{Al}_5\text{O}_{12}/\text{Ln}^{3+}$ (YAG/ Ln^{3+}), as well as for the barycenter positions of Ln^{3+} $4f^N$ configurations relative to the

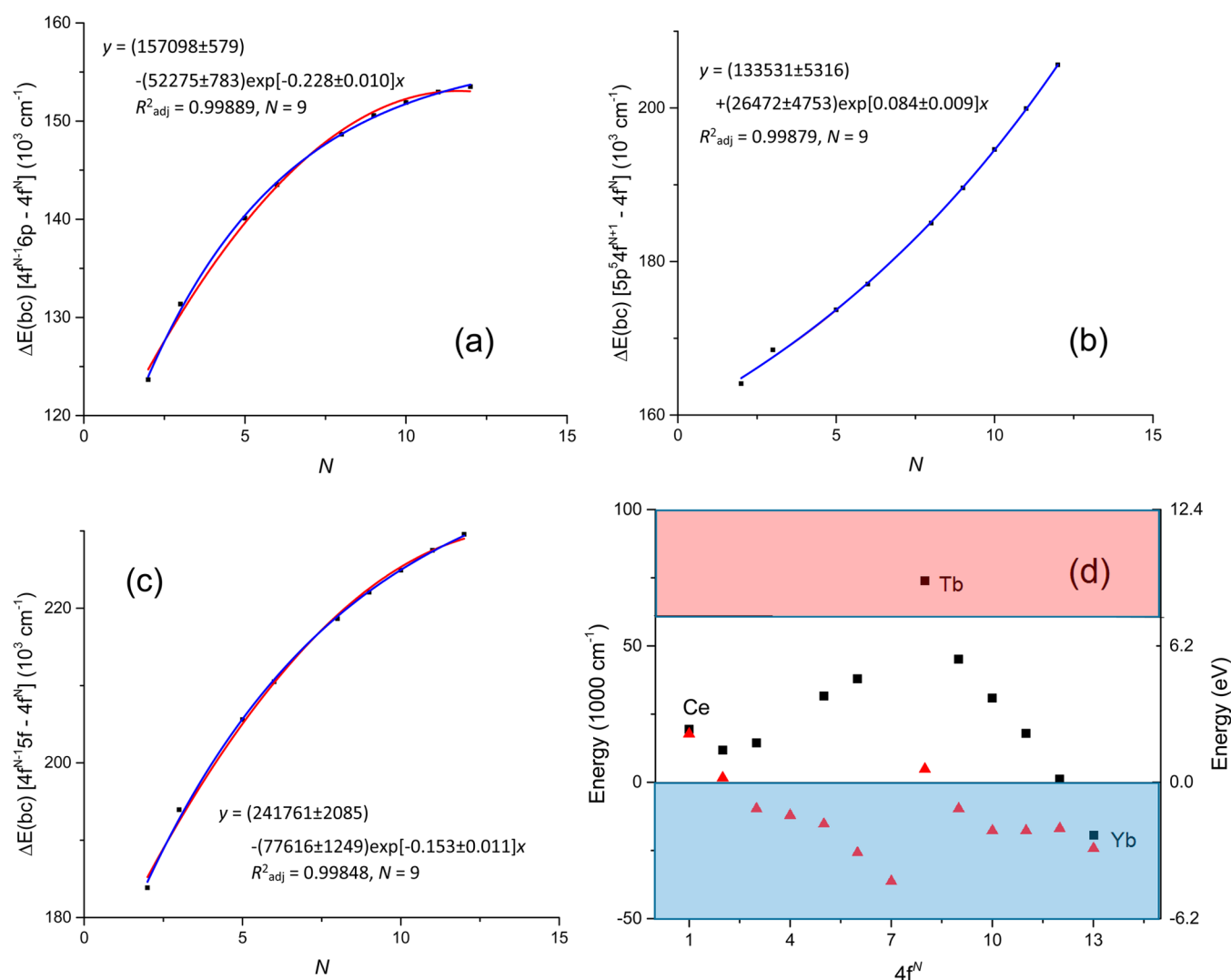


Figure 2. Calculated energy barycenters of excited configurations for Ln^{3+} systems with respect to those of $4f^N$: (a) $4f^{N-1}6p$; (b) $5p^5 4f^{N+1}$; (c) $4f^{N-1}5f$. The fitted equations (full blue lines) are indicated with N referring to the number of data in the fit, and the alternative fits using polynomials of order two are shown as dashed red lines in (a) and (c). (d) $4f^N$ barycenter (square data points) and lowest $4f^N$ energy level (triangular data points) of Ln^{3+} relative to the valence and conduction bands of YAG.

electronic ground states of these systems. The detailed calculation results are still being processed and will be reported elsewhere.

The differences in center-of-gravity energies between $4f^N$ and other configurations, $\Delta E(\text{bc})$, were calculated using Cowan's code,²¹ with the inclusion of approximate relativistic and correlation energy corrections.

3. RESULTS AND DISCUSSION

3.1. Calculation of Ground- and Excited-State Configuration Barycenter Energies. From the discussion in the Introduction, the most important excited electronic configurations of interest, with respect to CI with $4f^N$, are expected to be $4f^{N-1}6p$, $5p^5 4f^{N+1}$, and $4f^{N-1}5f$. The energy barycenters of these configurations, with respect to those of $4f^N$, $\Delta E(\text{bc})$, have been calculated using Cowan's code, and they are plotted in Figure 2a–c. The plots can be fitted almost equally well by exponential functions or by polynomials of order two, and the former are indicated.

The barycenters of $4f^N$ ground-state configurations were also calculated for YAG/ Ln^{3+} . The values increase, according to a

second-order polynomial, up to $\text{Ln} = \text{Gd}$ and then decrease. The values differ very little (<2%) from those given for $\text{Cs}_2\text{NaLnCl}_6$.²² The barycenters (denoted by squares) are plotted with respect to the valence and conduction bands²³ of the direct band gap insulator YAG in Figure 2d, in addition to the relative energies of the electronic ground states of Ln^{3+} (denoted by triangles). The $4f^6$ barycenter of Tb^{3+} lies in the conduction band, whereas the barycenters of other Ln^{3+} (except for $\text{Ln} = \text{Yb}$) lie in the band gap. The valence band (VB) of YAG is fairly deep ($\sim 6.5 \text{ eV}$), with mainly O-2p levels near the top.

3.2. Variation in Values of CI Parameters α , β , and γ . Our free ion calculation for Pr^{3+18} provided the fitted values (in cm^{-1}) of the parameters α and β of 23.93 ± 0.04 and -593 ± 2 , respectively. The values of the parameter γ , which is strongly correlated with F^2 , varied considerably depending upon the constraints of other parameters. For comparison of these figures, we calculate the corresponding values of α and β for YAG/ Pr^{3+} under various different fitting assumptions as 21.5 ± 0.3 and $-665 \pm 13 \text{ cm}^{-1}$, respectively, which indicate changes of between 10 and 12%. Such variations may be anticipated in

Table 1. Literature Values of CI Parameter α with Standard Deviations in Parentheses^a

Ln	4f ^N	Ln(OH ₂) _n ²⁴	LaCl ₃ ²⁵	LaF ₃ ²⁶	LiYF ₄ ²⁷	YAG
Pr	2	21.255(1.2)	22.84(0.94)	16.23(0.23)		21.84(0.14)
Nd	3	0.5611(1.4)	22.13(0.86)	21.34(0.14)	21.1(2.3)	20.9(0.1)
Pm	4	10.991(2.5)	20.92(0.51)			
Sm	5	22.25(1.3)	21.55(1.36)	20.16(0.89)		17.34(0.05)
Eu	6		16.82(2.21)		17.1(4.2)	
Gd	7		18.30(1.70)	18.92(0.83)		
Tb	8		16.73(1.66)	18.40(0.19)		
Dy	9	37.062(1.9)	17.46(1.32)	18.02(0.23)		
Ho	10	23.635(0.88)	17.33(0.95)	17.15(0.11)	16.1(1.6)	16.35(0.02)
Er	11	18.347(1.2)	16.06(1.79)	17.79(0.20)	20.0(5.2)	17.17(0.07)
Tm	12	14.677(4.2)	18.19(4.72)	17.26(0.30)	18.2(2.3)	13.62(0.18)

^aValues for YAG/Ln³⁺ are from the present study. All values are in cm⁻¹.

the comparison of free ion and solid-state data. The values of the CI parameters were found to be sensitive to the sampling of energy levels included in the data fit and hence to the degree of completeness of the energy level data set. For example, a fit to 126 levels of Er³⁺ in YAG/Er³⁺ gave $\alpha = 17.17 \pm 0.07$ cm⁻¹, whereas a fit to 45 middle levels of these gave $\alpha = 18.85 \pm 0.05$ cm⁻¹.

Many literature studies have based the parameters in the atomic Hamiltonian upon the values from the classic study of Carnall et al.²⁴ on aquo ions of Ln³⁺. In fact, the data sets were derived from the band centers in the broad, room-temperature spectra of Ln³⁺ in acid solutions, and the parameters do not represent “free ion” data because Ln³⁺ is coordinated by water molecules. The effects of the crystal field were not considered. The parameter values for α from this study,²⁴ which were listed to three decimal places even though the listed errors were more than 25% in one case, are shown in Table 1, and no overall trend is evident. We therefore instead consider analyses of individual crystal field levels, and the most comprehensive 4f^N energy level analyses for tripositive lanthanide ions that have been carried out include those for LaCl₃/Ln³⁺, LaF₃/Ln³⁺, and LiYF₄/Ln³⁺. The literature data for the parameter α for the chloride and fluoride systems are listed in Table 1 together with our values so far for YAG/Ln³⁺. More complete data are plotted in Figure 3a–c against the reciprocal of the energy barycenter difference between 4f^N and 4f^{N-1}6p. Each point is identified by the respective lanthanide ion and also by the percentage of states in the 4f^N configuration that were employed in the data fit. For example, the data point for Eu in Figure 3a comes from a fitting of only 58 energy levels from the entire 3003 in the 4f⁶ configuration (i.e., ~2%). The data point for Pr in Figure 3b, marked as a red cross, has been discarded because it appears to be anomalous. The bars for each point represent the inverse of the standard deviation of fitting, and these were employed in (a) and (b) for direct weighting in the linear regressions, which gave the results

For LaCl₃/Ln³⁺

$$\alpha = -(11.4 \pm 4.4) + (4.3 \pm 0.6)[10^6/\Delta E(\text{bc})]$$

$$(R_{\text{adj}}^2 = 0.8317, N = 8) \quad (3)$$

For LaF₃/Ln³⁺

$$\alpha = -(7.1 \pm 2.4) + (3.8 \pm 0.3)[10^6/\Delta E(\text{bc})]$$

$$(R_{\text{adj}}^2 = 0.9435, N = 8) \quad (4)$$

For YAG/Ln³⁺

$$\alpha = -(8.0 \pm 6.0) + (3.7 \pm 0.9)[10^6/\Delta E(\text{bc})]$$

$$(R_{\text{adj}}^2 = 0.7671, N = 6) \quad (5)$$

The regression eqs 3–5 are similar, also taking into account the incompleteness of data sets, and show that about 80–90% of the variance of α can be accounted for by CI with the single lowest same-parity configuration. Notice that the free ion barycenters have been employed in these plots, although the parameters α are taken from crystal data. It is assumed that the scaling of energy differences from the free ion to the crystals would not greatly affect the above conclusion. Morrison et al. have calculated the contributions to the parameter α of Pr³⁺ using second-order perturbation theory.²⁸ The contributions to bound states were dominated by 4d⁸4f⁴, but these were largely canceled by excitations of one particle to the continuum. The contributions did not take into account those from the lowest same-parity configuration, 4f6p, as studied herein. Copland et al. also calculated the contributions to α for Pr²⁺ and Pr³⁺ and found that the 4f² → 4f6p contribution was unimportant.²⁹ A review of the contributions may be timely in view of our findings.

Values of the fitted parameter β are listed in Table 2 and plotted in Figure 4a. There is no clear overall trend. Consideration of only the values for LaCl₃/Ln³⁺ (with those for Ln = Sm and Tm discarded) and YAG/Ln³⁺ yields a linear plot against $[10^6/\Delta E(\text{bc})]$ with a slope of -65 ($R_{\text{adj}}^2 = 0.5086$, $N = 15$). The parameter γ has been constrained in many calculations because it varies wildly due to the strong correlation with the Slater parameter F^2 . Data from LaCl₃/Ln³⁺ and LaF₃/Ln³⁺ are plotted in Figure 4b, and the linear fit has a slope of -268 ($R_{\text{adj}}^2 = 0.4344$, $N = 14$). Thus, in both cases of the variations of β and γ , it appears that the slope has an opposite sign to that of α .

Finally, it is noted again that the interaction of 4f^N with 4f^{N-1}6p and 4f^{N+1}5p⁵ is described not only by two-electron but also by three-electron operators. The latter interactions have not been considered in this work.

3.3. Crystal Field Effects and CI. By contrast to the same-parity Coulombic CI discussed above, in the solid-state, the interaction can also occur with other configurations via the crystal field operator, and it is timely to include some comments herein, although no further research in this area has yet been performed by our group.

This effect was set out in a general sense by Rajnak and Wybourne³⁰ with the use of second-order perturbation theory

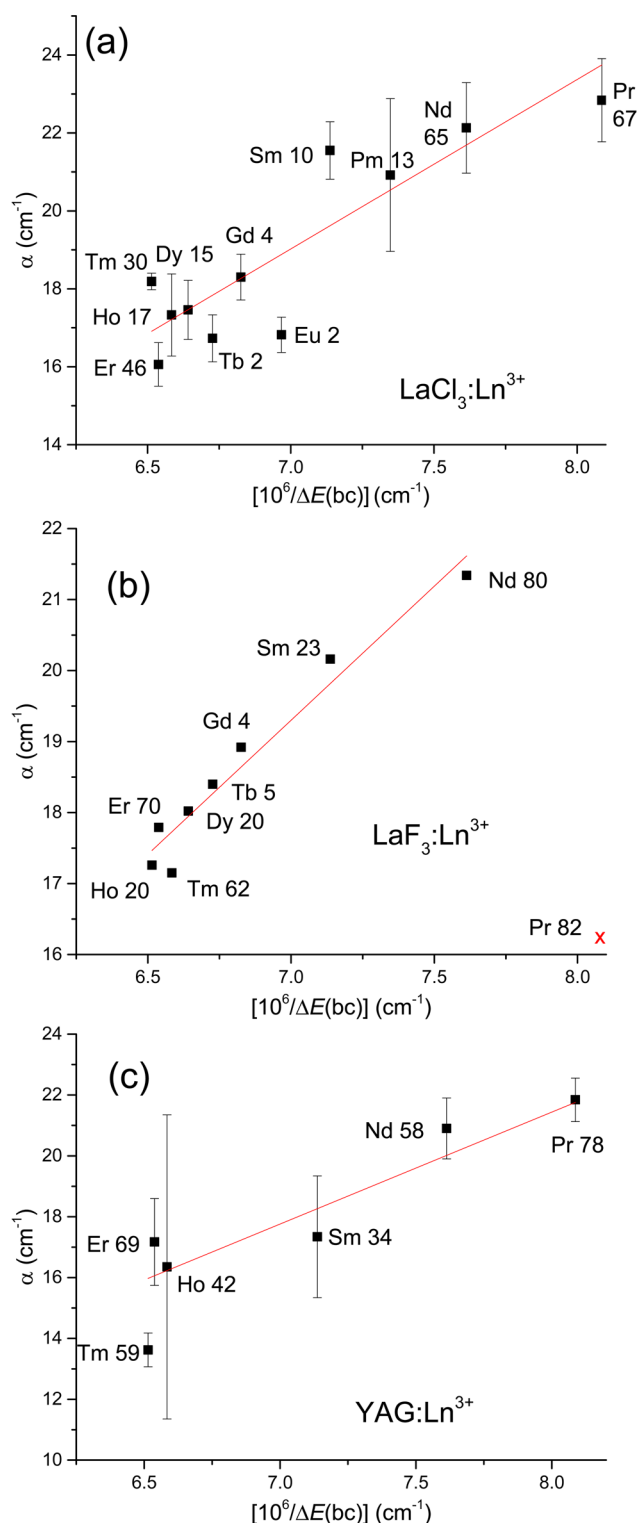


Figure 3. Plot of fitted values of α against $[10^6/\Delta E(\text{bc})]$, where $\Delta E(\text{bc})$ is the energy difference between the barycenters of the $4f^N$ and $4f^{N-1}6p$ configurations: (a) $\text{LnCl}_3/\text{Ln}^{3+}$; (b) $\text{LnF}_3/\text{Ln}^{3+}$; (c) $\text{YAG}/\text{Ln}^{3+}$. Data are from Table 1. Refer to the text for explanation.

and the consideration of configuration barycenter differences. These authors pointed out that because the crystal field operator is a single-particle operator, it can only couple configurations that differ from $4f^N$ by the excitation of a single electron, that is, such as $4f^N 5p^5 6p$, $4f^N 5p^5 5d$, $4f^{N-1} 6p$, $4f^{N-1} 5d$, and $4f^{N+1} 5p^5$. The different configurations exert different effects

Table 2. Rounded Literature Values (in cm^{-1}) of CI Parameter β with Standard Deviations in Parentheses^a

Ln	$4f^N$	LaCl_3^{25}	LaF_3^{26}	LiYF_4^{27}	YAG
Pr	2	−682(8)	−567(15)	−653(22)	−676(9)2
Nd	3	−657(6)	−593(8)	−574(17)	−643(4)
Pm	4	−645(3)			
Sm	5	−717(8)	−567(8)		−567(2)
Eu	6	−630(20)		−646(24)	
Gd	7	−639(18)			
Tb	8	−571(15)	−591(29)		
Dy	9	−608(8)	−633(10)		
Ho	10	−629(6)	−608(6)	−529(7)	−587(1)
Er	11	−607(11)	−582(10)	−589(26)	−614(3)
Tm	12	−745(23)	−625(15)	−680(14)	−524(7)

^aValues for YAG/ Ln^{3+} are from the present study.

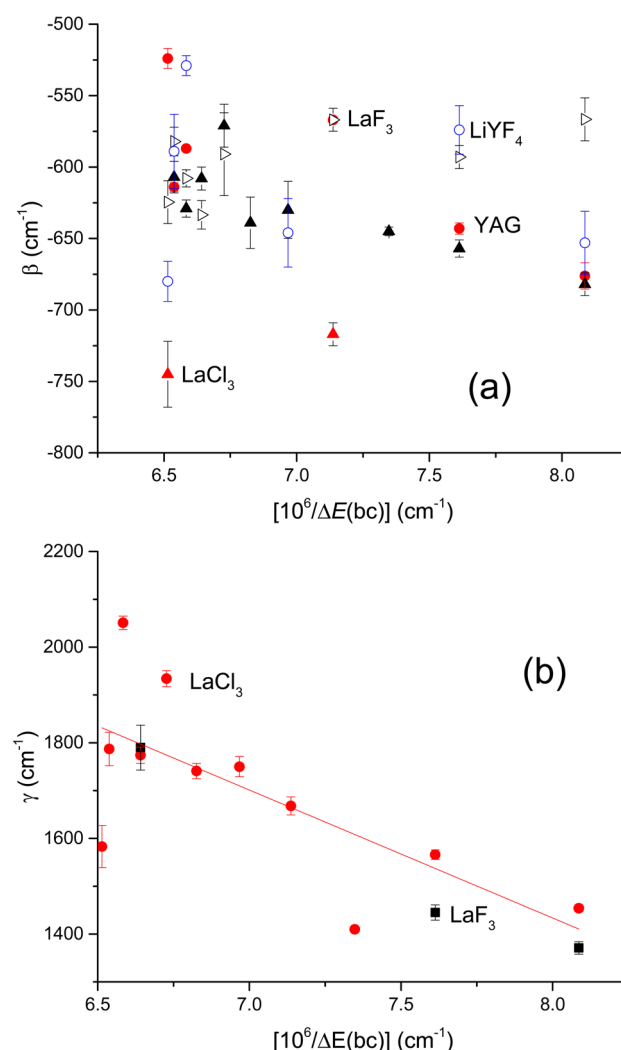


Figure 4. (a) Plot of fitted values of β against $[10^6/\Delta E(\text{bc})]$, where $\Delta E(\text{bc})$ is the energy difference between the barycenters of the $4f^N$ and $4f^{N-1}6p$ configurations. The data points are identified for $\text{LnCl}_3/\text{Ln}^{3+}$, $\text{LnF}_3/\text{Ln}^{3+}$, $\text{LiYF}_4/\text{Ln}^{3+}$, and $\text{YAG}/\text{Ln}^{3+}$, from Table 2. (b) Corresponding plot for the parameter γ with data from $\text{LaCl}_3/\text{Ln}^{3+}$ and $\text{LaF}_3/\text{Ln}^{3+}$,²⁶ as identified. In both of these plots, the vertical bars represent stated standard deviations.

upon the crystal field parameters, as detailed in ref 30, with scaling in many cases, but different parameters need to be

associated with different multiplets for mixing with $4f^{N-1}nl$. The second-order CI can occur via the crystal field alone or by an electrostatically correlated crystal field interaction (i.e., the CI involves Coulomb interaction and the crystal field potential through a perturbation approach).

It has long been recognized that accurate fitting of different multiplets of Ln^{3+} in crystals requires different sets of crystal field parameters. In particular, the crystal field splittings of some J -multiplets of Ln^{3+} are anomalous, such as those for $\text{Pr}^{3+} \text{G}_4$, $^1\text{D}_2$; Nd^{3+} and $\text{Er}^{3+} \text{H}(2)_{11/2}$. One approach to parametrize these effects has been to include various correlation crystal field corrections with two-particle operators into the Hamiltonian. However, the choice of term is rather arbitrary from the large number of possibilities (637 for C_1 site symmetry of Ln^{3+} and even 41 for O_h site symmetry), and the corrections often do not give accurate results for energy level locations.³¹ An alternative approach to the inclusion of crystal field interaction was made by Garcia and Faucher,³² who used a complete Hamiltonian in an extended basis that included the two interacting configurations. The anomalous splitting of the $\text{Pr}^{3+} \text{D}_2$ multiplet via the interaction of odd-rank crystal field parameters with the $4f5d$ configuration was well-explained (and subsequently amplified through the inclusion of further configurations³³). The essential point is that because these configurations are fairly close together, the energy denominators for the interaction now refer to specific multiplet–multiplet energy separations rather than to barycenter differences. The mixing, by the odd-rank crystal field operators, was deemed to be of importance because it is the same mechanism that gives rise to the $4f^N$ – $4f^N$ spectral intensities of Ln^{3+} in most crystals.

In the cases of Ln^{3+} situated at centrosymmetric sites, because the crystal field parameters are of even rank, the interaction must occur with configurations of the same parity. Hence, a marked improvement in the energy level fitting of Pr^{3+} in $\text{Cs}_2\text{NaPrCl}_6$ was achieved by explicitly including the $4f6p$ configuration into the Hamiltonian of $4f^2$.³⁴ In the case of the $\text{Tm}^{3+} 4f^{12}$ in $\text{Cs}_2\text{NaTmCl}_6$, the interacting configuration was taken as the charge-transfer configuration $4f^{13}3p^5$,³⁵ as analogously for the $\text{Er}^{3+} 4f^{11}$ system in $\text{Cs}_2\text{NaErCl}_6$.³⁶ The results in the present study show that for Tm^{3+} , the $4f^{12}$ barycenter for $13 \text{ } ^{2S+1}L_J$ levels is at 16663 cm^{-1} , whereas those for the $4f^{13}5p^5$ and the $4f^{14}6p$ configurations are at 223277 and 170141 cm^{-1} , respectively. By contrast, the charge-transfer configuration $\text{Tm}^{2+} 4f^{13} + \text{VB}(\text{h}^+)$ commences at about 47600 cm^{-1} above the top of the VB. Hence, the crystal field interaction will depend upon the ligand type and metal–ligand distance. The energy level fits in refs 34–36 are convincing but still pose one unresolved problem. The fitted $4f^N$ crystal field parameters with the inclusion of CI-assisted crystal field calculations exhibit great changes from the values from $4f^N$ calculations alone. This problem needs to be investigated. The solution may be to perform fits of the energy levels with the two configurations included but with the $4f$ crystal field parameters held at fixed values in each fit. On the other hand, the fitted values of the CI parameters α , β , and γ do not exhibit much change from their $4f^N$ -fitted values and the free ion values. The inclusion of the metal–ligand charge-transfer configuration would be expected to lead to changes from the free ion values and also provide abrupt changes in the trend across the Ln^{3+} series.

3.4. Electrostatically Correlated Spin–Orbit Interaction. Judd et al. have given the equation for the parameter P^2 ,

and assuming that the CI occurs only between $4f^N$ and $4f^{N-1}5f$, it becomes¹⁶

$$P^2 = 6 \times \zeta(4f5f) \times R^2(4f4f, 4f5f) / \Delta E(\text{bc})(4f5f) \quad (6)$$

where $\zeta(4f5f)$ and $R^2(4f4f, 4f5f)$ are the off-diagonal radial integrals of the spin–orbit and Coulomb interaction, respectively, and $\Delta E(\text{bc})(4f5f)$ is the positive barycenter difference between the $4f^N$ and $4f^{N-1}5f$ configurations,³⁷ as in Figure 2c. The values of P^2 from the analysis of $\text{LaCl}_3/\text{Ln}^{3+25}$ are plotted against $[\Delta E(\text{bc})4f5f]$ in Figure 5. The data points

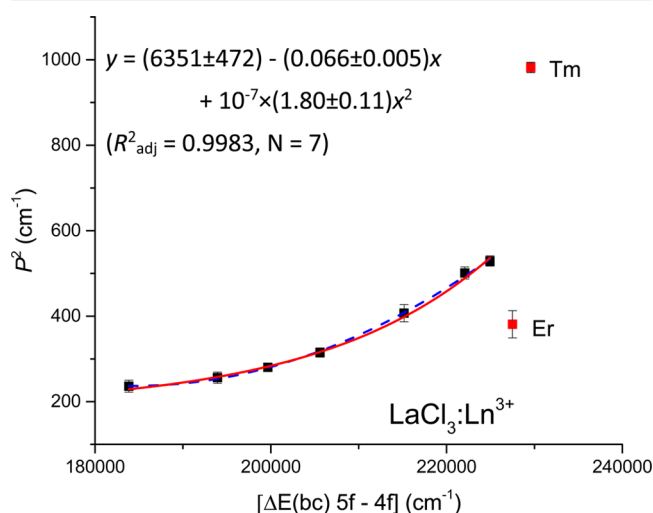


Figure 5. Plot of the parameter values P^2 from the analyses of $\text{LaCl}_3/\text{Ln}^{3+}$ data sets versus the difference in barycenter energy of the relevant $4f$ and $5f$ configurations. Refer to the text for explanation.

for Er^{3+} ($P^2 = 381 \pm 32 \text{ cm}^{-1}$) and Tm^{3+} ($P^2 = 982 \pm 12 \text{ cm}^{-1}$) do not follow the trend of the other Ln^{3+} and are marked as red squares. We recently reported the energy data set analyses for $\text{LaCl}_3/\text{Ln}^{3+}$ ($\text{Ln} = \text{Pr}, \text{Nd}, \text{Er}$),²⁰ and our fitted values for Pr and Nd are reasonably similar (differing by 12.6 and 0.3%, respectively) to those of ref 25, but our fitted value for Er^{3+} ($727 \pm 20 \text{ cm}^{-1}$) differs markedly. We have therefore omitted these two points. The graph can be fitted almost equally well by an exponential (red; full line) or second-order polynomial (black; dashed line) function, and the equation for the latter is indicated. Notice that the trend of P^2 across the Ln^{3+} series is actually an increase; the radial integrals decrease by $\sim 40\%$, the spin–orbit integrals ζ_{4f} increase by $\sim 200\%$, and the energy barycenter difference $\Delta E(\text{bc})(4f5f)$ increases by $< 30\%$.

With the use of the approximation $\zeta(4f5f) \approx [\zeta(4f) \times \zeta(5f)]^{1/2}$, the contributions to the P^k from bound states have been calculated using eq 6 with data from Cowan's code, and the relevant results are listed in Table 3. The barycenter energy differences $\Delta E(\text{bc})(4fnf)$ rapidly converge with increasing n , and the spin–orbit constants $\zeta(nf)$ decrease when the radial orbit expands. The contributions to P^k decrease with increasing n , with the totals for $n = 5$ – 9 being (in cm^{-1}) 174, 117, and 86 for $k = 2, 4$, and 6 , respectively. The contributions of the $n = 5$ values to the total for P^k are only between 54 and 61%. The calculated ratios $P^2/P^4/P^6$ from the totals are 1:0.67:0.49. The experimental fitted value of P^2 for the Pr^{3+} free ion is 204.9 ± 2.3 ,¹⁸ which is only 20% above the calculated value, with the remaining contributions assigned to excitations to continuum states. The literature values of P^k for Pr^{3+} in crystals vary considerably, however, with some even being negative (e.g.,

Table 3. Contributions to P^k from Bound States^a

Config ⁿ 4f ⁿ f	ζ_{4f}	ζ_{nf}	$\zeta(4f,nf)$	$\Delta E(bc)$ (nf–4f)	R^2	R^4	R^6	P^2	P^4	P^6
4f ²	827	827	827	0						
4f5f	921	40	193	186927	15347	10238	7525	95	63	47
4f6f	922	22	142	227454	10444	7017	5174	39	26	19
4f7f	923	13	109	249031	7731	5211	3847	20	14	10
4f8f	923	8	87	262000	6026	4069	3007	12	8	6
4f9f	923	6	72	270400	4873	3294	2435	8	5	4

^aThe values were generated from Cowan's code with scaling factors of 0.7 for Slater parameters and 0.99 for spin–orbit coupling constants. All values are in cm^{−1}; R^k refers to $R^k(4f4f, 4f5f)$. Configⁿ is the configuration.

−88.6 ± 47 cm^{−1} for LaF₃/Pr³⁺²⁶) and the ratios for $P^2/P^4/P^6$ also varying (e.g., for LaF₃/Pr³⁺, 1.0:0.5:0.1²⁶). Evidently, the magnetic parameters are absorbing errors either from incorrect spectral assignments and/or other incorrect parameter values in such cases. Our fitted value for LaCl₃/Pr³⁺²⁰ of 265.7 ± 7.3 cm^{−1} is rather higher than the free ion value and supports other contributions to P^2 related to the crystalline state. This participation of such contributions is emphasized from the fitted value of P^2 between 498 and 526 cm^{−1} in our energy level analyses of YAG/Pr³⁺.

4. CONCLUSIONS

This work has highlighted, but not solved, some of the questions concerning the interaction of the 4f^N configuration with other excited ones. Unfortunately, nearly all published crystal field analyses of Ln³⁺ energy level data sets have flaws. This arises not only from the use of incorrect matrix elements or the neglect of spin–spin interactions²⁰ but also because the energy level data sets are incomplete or assignments of the raw data are incorrect or inaccurate. Hence, some parameters that describe second-order effects are forced to absorb errors in other parameter values, and often, a strong intercorrelation exists between the parameters. The need for more complete and accurate analyses is stressed in order to achieve reliable fitted values of the energy parameters of second-order importance, and we are embarking upon this project.

The contributions to the parameter α show that the nearest same-parity configuration is of most importance. The changes in barycenter energy difference are not major for Ln³⁺, so that this parameter does not exhibit a wide variation in magnitude across the Ln³⁺ series. Furthermore, it appears that values of α from free ion spectra are not drastically different from those of crystal field energy level fittings. At least the present study provides evidence to recognize anomalous values of the parameters α and β from energy level fittings. The behavior of α across the Ln³⁺ series contrasts with that for the four 4f² ions recently studied, where the nature of the interacting configuration changes markedly and produces very different values of α .¹⁸

It has been found that the type and charge of the coordinated ligand with Ln³⁺ make substantial changes in the values of the P^k parameters. Indeed, an outstanding problem in the crystal-field-assisted CI model has been remarked upon with the view of future progress in its solution.

AUTHOR INFORMATION

Corresponding Author

*E-mail: peter.a.tanner@gmail.com. Tel.: (852) 90290610.

Notes

The authors declare no competing financial interest.

ACKNOWLEDGMENTS

Financial support from the National Natural Science Foundation of China (Grant 11174005) is gratefully acknowledged by L.N.

REFERENCES

- (1) Froese Fischer, C.; Brage, T.; Jönsson, P. *Computational Atomic Structure. An MCHF Approach*; Institute of Physics Publishing; Bristol, U.K., 2000. pp 1–279.
- (2) Krośnicki, M.; Kędziorowski, A.; Seijo, L.; Barandiarán, Z. Ab Initio Theoretical Study on the 4f² and 4f5d Electronic Manifolds of Cubic Defects in CaF₂:Pr³⁺. *J. Phys. Chem. A* **2014**, *118*, 358–368.
- (3) Belén Muñoz-García, A.; Seijo, L. Ce and La Single- and Double-Substitutional Defects in Yttrium Aluminium Garnet: First-Principles Study. *J. Phys. Chem. A* **2011**, *115*, 815–823.
- (4) Trees, R. E.; Jørgensen, C. K. Parameters α and β in the Spectra of the Iron Group. *Phys. Rev.* **1961**, *123*, 1278–1280.
- (5) Rajnak, K.; Wybourne, B. G. Configuration Interaction Effects in f^N Configurations. *Phys. Rev.* **1963**, *132*, 280–290.
- (6) van Pieterse, L.; Reid, M. F.; Wegh, R. T.; Meijerink, A. 4fⁿ–4f^{n−1}5d Transitions of the Trivalent Lanthanides: Experiment and Theory. *J. Lumin.* **2001**, *94–95*, 79–83.
- (7) Malkin, B. Z.; Solov'yev, O. V.; Malishev, A. Yu.; Saikin, S. K. Theoretical Studies of Electron-Vibrational 4fⁿ–4f^{n−1}5d Spectra in LiYF₄:RE³⁺ Crystals. *J. Lumin.* **2007**, *125*, 175–183.
- (8) Duan, C.-K.; Tanner, P. A.; Meijerink, A.; Babin, V. Synchrotron Excitation, Emission and Theoretical Simulation of Lanthanide Ions in Hexachloroelpasolite Crystals. *J. Phys.: Condens. Matter* **2009**, *21*, 395501/1–395501/9.
- (9) Judd, B. R. Three-Particle Operators for Equivalent Electrons. *Phys. Rev.* **1966**, *141*, 4–14.
- (10) Judd, B. R. *Operator Techniques in Atomic Spectroscopy*; McGraw-Hill; New York, 1963; Chapter 5.
- (11) Wybourne, B. G. *Spectroscopic Properties of Rare Earths*; Interscience: London, 1965.
- (12) Enzonga Yoca, S.; Quinet, P. Relativistic Hartree–Fock Calculations of Transition Rates for Allowed and Forbidden Lines in Nd IV. *J. Phys. B: At. Mol. Opt. Phys.* **2014**, *47*, 035002/1–035002/15.
- (13) Meftah, A.; Wyart, J.-F.; Champion, N.; Tchang-Brillet, W.-Ü. L. Observation and Interpretation of the Tm³⁺ Free Ion Spectrum. *Eur. Phys. J. D* **2007**, *44*, 35–45.
- (14) Kramida, A.; Raichenko, Yu.; Reader, J. NIST ASD Team, NIST, *Atomic Spectra Database* version 5.0, [On-line]. Available <http://physics.nist.gov/asd> (accessed Sept. 5, 2013).
- (15) Rajnak, K.; Wybourne, B. G. Electrostatically-Correlated Spin–Orbit Interactions in f^N -Type Configurations. *Phys. Rev.* **1964**, *134*, A596–A600.
- (16) Judd, B. R.; Crosswhite, H. M.; Crosswhite, H. Intra-Atomic Magnetic Interactions for l Electrons. *Phys. Rev.* **1968**, *169*, 130–138.
- (17) Crosswhite, H. M.; Crosswhite, H. Parametric Model for f -Shell Configurations. I. The Effective-Operator Hamiltonian. *J. Opt. Soc. Am. B* **1984**, *1*, 246–254.
- (18) Yeung, Y.-Y.; Tanner, P. A. Parametrization of Free Ion Levels of Four Isoelectronic 4f² Systems: Insights into Configuration Interaction Parameters. *Chem. Phys. Lett.* **2013**, *590*, 46–51.

- (19) Yeung, Y.-Y. Reduced Matrix Elements of Spin–Spin Interactions for the Atomic f-Electron Configurations. *Atomic Data Nucl. Tables* **2014**, *100*, 536–576.
- (20) Yeung, Y.-Y.; Tanner, P. A. New Analyses of Energy Level Datasets for $\text{LaCl}_3/\text{Ln}^{3+}$ ($\text{Ln} = \text{Pr}, \text{Nd}, \text{Er}$). *J. Alloys Compd.* **2013**, *575*, 54–60.
- (21) Cowan, R. D. *The Theory of Atomic Structure and Spectra*; University of California: Berkeley, CA, 1981.
- (22) Duan, C.-K.; Tanner, P. A. What Use are Crystal Field Parameters? A Chemist's Viewpoint. *J. Phys. Chem. A* **2010**, *114*, 6055–6062.
- (23) Thiel, C. W.; Cruguel, H.; Wu, H.; Sun, Y.; Lapeyre, G. J.; Cone, R. L.; Equall, R.; Macfarlane, R. M. Systematics of 4f Electron Energies Relative to Host Bands by Resonant Photoemission of Rare Earth Ions in Aluminium Garnets. *Phys. Rev. B* **2001**, *64*, 085107/1–085107/13.
- (24) Carnall, W. T.; Fields, P. R.; Rajnak, K. Electronic Energy Levels in the Trivalent Lanthanide Aquo Ions. I. Pr^{3+} , Nd^{3+} , Pm^{3+} , Sm^{3+} , Dy^{3+} , Ho^{3+} , Er^{3+} , and Tm^{3+} . *J. Chem. Phys.* **1968**, *44*, 4424–4442.
- (25) Jayasankar, C. K.; Richardson, F. S.; Reid, M. F. Phenomenological Spin-Correlated Crystal-Field Analyses of Energy Levels in $\text{Ln}^{3+}:\text{LaCl}_3$ Systems. *J. Less-Common Met.* **1989**, *148*, 289–296.
- (26) Carnall, W. T.; Goodman, G. L.; Rajnak, K.; Rana, R. S. A Systematic Analysis of the Spectra of the Lanthanides Doped into Single Crystal LaF_3 . *J. Chem. Phys.* **1989**, *90*, 3443–3457.
- (27) Jayasankar, C. K.; Reid, M. F.; Richardson, F. S. Comparative Crystal-Field Analyses of $4f^N$ Energy Levels in $\text{LiYF}_4/\text{Ln}^{3+}$ Systems. *Phys. Status Solidi B* **1989**, *155*, 559–569.
- (28) Morrison, J.; Rajnak, K.; Wilson, M. Evaluation of Effective Operators for Configuration Interaction. *J. Phys. (Paris)* **1970**, *31* (C4), 167–171.
- (29) Copland, G. M.; Newman, G. J.; Taylor, C. D. Configuration Interaction in Rare Earth Ions: III. Trees Parameters for Pr^{2+} and Pr^{3+} . *J. Phys. B: At. Mol. Phys.* **1971**, *4*, 1605–1610.
- (30) Rajnak, K.; Wybourne, B. G. Configuration Interaction in Crystal Field Theory. *J. Chem. Phys.* **1964**, *41*, 565–569.
- (31) Burdick, G. W.; Richardson, F. S. Correlation-Crystal-Field “ δ -Function” Analysis of Pr^{3+} ($4f^2$) Energy-Level Structure. *J. Alloys Compd.* **1997**, *250*, 293–296.
- (32) Garcia, D.; Faucher, M. An Explanation of the $^1\text{D}_2$ Anomalous Crystal Field Splitting in PrCl_3 . *J. Chem. Phys.* **1989**, *90*, 5280–5283.
- (33) Garcia, D.; Faucher, M. A Full Calculation of Multiconfiguration Interaction Effects up to 120000 cm^{-1} (15 eV) on the Ground Configuration State Levels of PrCl_3 . Zeeman Effect Interpretation. *J. Chem. Phys.* **1989**, *91*, 7461–7466.
- (34) Tanner, P. A.; Mak, C. S. K.; Faucher, M. D. Configuration Interaction of Pr^{3+} in PrCl_6^{3-} . *J. Chem. Phys.* **2001**, *114*, 10860–10871.
- (35) Faucher, M. D.; Tanner, P. A.; Mak, C. S. K. Electronic Spectra and Configuration Interaction of Tm^{3+} in TmCl_6^{3-} . *J. Phys. Chem. A* **2004**, *108*, 5278–5287.
- (36) Faucher, M. D.; Tanner, P. A. Full Configuration Interaction of Er^{3+} and Covalency in the Elpasolite Compound $\text{Cs}_2\text{NaErCl}_6$. *Mol. Phys.* **2003**, *101*, 983–992.
- (37) Copland, G. M.; Newman, D. J.; Taylor, C. D. Configuration Interaction in Rare Earth Ions: II. Magnetic Interactions. *J. Phys. B: At. Mol. Phys.* **1971**, *4*, 1388–1392.